

ALIGNMENTS OF THE DOMINANT GALAXIES IN POOR CLUSTERS

TODD M. FULLER¹ AND MICHAEL J. WEST²

Department of Astronomy and Physics, Saint Mary's University, Halifax, Nova Scotia B3H 3C3, Canada; fuller@phobos.astro.uwo.ca,
west@ap.stmarys.ca

AND

TERRY J. BRIDGES²

Institute of Astronomy, Cambridge, England, UK; tjb@ast.cam.ac.uk

Received 1998 July 27; accepted 1999 February 9

ABSTRACT

We have examined the orientations of brightest cluster galaxies (BCGs) in poor MKW (Morgan, Kayser, and White) and AWM (Albert, White, and Morgan) clusters and find that, like their counterparts in richer Abell clusters, poor cluster BCGs exhibit a strong propensity to be aligned with the principal axes of their host clusters as well as the surrounding distribution of nearby ($\leq 20 h^{-1}$ Mpc) Abell clusters. The processes responsible for dominant galaxy alignments are therefore independent of cluster richness. We argue that these alignments most likely arise from anisotropic infall of material into clusters along large-scale filaments.

Subject headings: galaxies: clusters: general — galaxies: structure

1. INTRODUCTION

The orientation of galaxies is one more piece to be fit into the puzzle of galaxy formation. Statistically significant evidence for alignments between the principal axes of rich Abell clusters and the major axes of their dominant galaxies (hereafter referred to as BCGs [brightest cluster galaxies]) has been reported by numerous authors (Sastry 1968; Carter & Metcalfe 1980; Struble & Peebles 1985; Rhee & Katgert 1987; Lambas, Groth, & Peebles 1988). Struble (1990) and Trevese, Cirimele, & Flin (1992) found that the BCG major axis is also aligned with the line joining the first and second brightest galaxies and that the second brightest galaxy is weakly aligned with the first. There is also solid evidence that BCGs and their parent clusters are aligned with the distribution of neighboring clusters on scales up to several tens of Mpc (Binggeli 1982; Lambas et al. 1990; West 1994).³ For instance, West (1994) finds that there is significant alignment (at $> 99.9\%$ confidence) of the innermost regions ($\leq 2 h^{-1}$ kpc) of 147 Abell cluster BCGs with the distribution of neighboring rich clusters out to $10 h^{-1}$ Mpc.

While many studies have been done, they have focused almost exclusively on rich clusters, so the effect of cluster environment on the alignment effects is not known. In order to investigate whether cluster richness influences the alignment effects, we have obtained CCD images of the BCGs of some poor clusters. Morgan, Kayser, & White (1975, hereafter MKW) and later Albert, White, & Morgan (1977, AWM) cataloged 23 candidate BCGs located in poor clusters. These poor clusters contain a few tens of bright galaxies and have virial masses of 10^{13} – $10^{14} M_{\odot}$ (e.g., Beers et

al. 1995), compared with 10^{14} – $10^{15} M_{\odot}$ for rich Abell clusters (e.g., Carlberg et al. 1996). Beers et al. (1995) find a median velocity dispersion of 336 km s^{-1} for 21 MKW/AWM poor clusters, about half that found in rich clusters (e.g., Zabludoff et al. 1990).

Flin et al. (1995) examined the MKW and AWM poor clusters for alignments between the parent cluster position angle and the position angles of the two brightest galaxies, and they found an alignment for the first brightest galaxies but not the second. Their observations were taken in 1986 with a 105 cm Schmidt telescope using photographic plates, and galaxy and cluster orientations were estimated by eye. Our study improves considerably on this previous work, since CCDs are much more sensitive and have improved linearity over photographic plates; they thus capture faint features more reliably. Also, our use of automated surface photometry procedures allow a more accurate determination of galaxy position angles. Using these data, we have investigated whether poor cluster BCGs are aligned with their host cluster and whether they are also aligned on larger scales with the distribution of surrounding Abell clusters.

Our observations and data reductions are described in the following section. In § 3 we examine the evidence for alignments of BCGs in poor clusters, and in § 4 we discuss the theoretical implications of our results.

2. OBSERVATIONS AND DATA REDUCTION

Images of BCGs in 21 of the 23 MKW/AWM clusters were obtained using the 1.0 m Jacobus Kapteyn Telescope (JKT) during an observing run in 1994 April and another in 1995 April. With the JKT in its f/15.0 configuration, the image scale of $0''.33$ and CCD size of 1124×1124 yielded a field of $6''.2 \times 6''.2$. We obtained 900 s *V*-band images in the first run and 900 s *B* and/or 600 s *R* images in the second.

The data were preprocessed (bias-subtracted, flat-fielded, and trimmed) using the IRAF CCDPROC package. Flat-fielding was performed using both twilight flats and dark sky flats, and the residual gradients in the final images were

¹ Present address: Department of Physics and Astronomy, University of Western Ontario, London, Ontario N6A 3K7, Canada.

² Visiting Observer, Jacobus Kapteyn Telescope (JKT). The JKT is operated on the island of La Palma by the Isaac Newton Group in the Spanish Observatorio del Roque de los Muchachos of the Instituto de Astrofísica de Canarias.

³ We adopt $H_0 = 100 \text{ h km s}^{-1} \text{ Mpc}^{-1}$ in this paper.

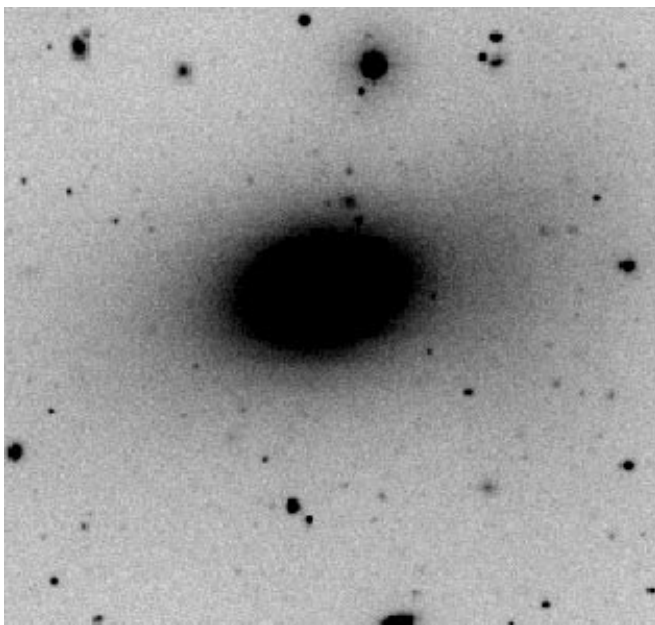


FIG. 1a

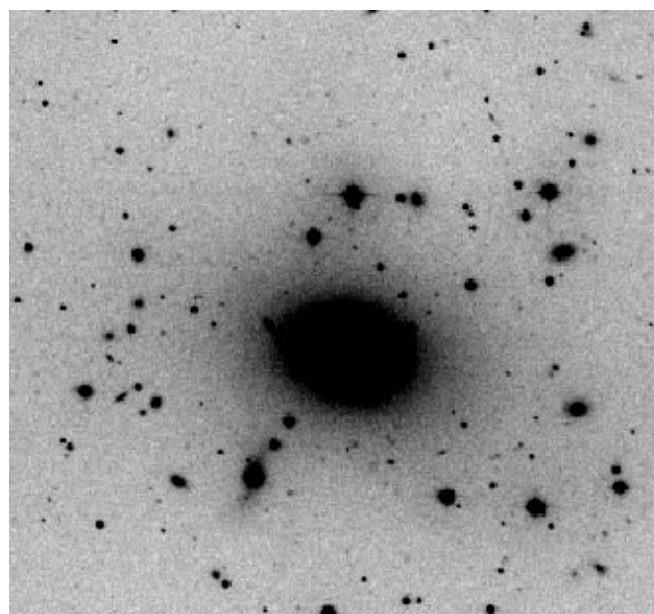


FIG. 1b

FIG. 1.—JKT *B* images of two poor cluster BCGs: (a) MKW 4 and (b) AWM 5

about 1.0% of the sky intensity. Contaminating objects (e.g., stars and cluster and background galaxies) were identified by eye and masked using generous radii. Figure 1 shows images of two galaxies in our sample.

The BCG position angles were measured with the STSDAS task ELLIPSE. This task uses the iterative method of Jedrzejewski (1987) to fit isophotal ellipses to galaxies. The user supplies initial estimates for the position angle, ellipticity, and ellipse center and specifies the final semimajor axis distance. The routine samples the images along an elliptical path and produces a one-dimensional intensity distribution as a function of the ellipse eccentric anomaly, E . The Fourier harmonics of the distribution are fitted by least squares to the function

$$y = y_0 + A_1 \sin(E) + B_1 \cos(E) + A_2 \sin(2E) + B_2 \cos(2E).$$

Next, the five ellipse parameters are adjusted by a correction found from the amplitudes A_1 , B_1 , A_2 , and B_2 . The parameter with the largest amplitude is varied, a new elliptical path is chosen, and the image is resampled. The task stops after a user-specified number of iterations or after the solution has converged, and the best-fitting ellipse is given by the parameters that produced the lowest absolute values of the harmonic amplitude. The output consists of the five ellipse parameters (x and y centroids, ellipticity, position angle, and axis length) plus higher order harmonics characterizing the departures from purely elliptical isophotes. The routine is fairly insensitive to the initial estimates; the deviations incurred here are much smaller than the variation in the position angle with radius.

3. ANALYSIS

The position angles listed in Table 1 were averaged over radii less than 6 kpc, where the isophote intensity was high.

The errors given are one standard deviation of the mean. The central few arcseconds were excluded, since seeing effects become stronger in the core and tend to make the isophotes round. For five galaxies (MKW 2, 2S, 3S, 4, and AWM 5) we obtained both *B* and *R* data, and the position angles given are average values. Figures 2 and 3 show the ellipticity and position angle profiles for a sample of the poor cluster BCGs. None of the galaxies in this study dis-

TABLE 1
POSITION ANGLES

| Cluster | θ_{BCG}^a (deg) | BCG Ellipticity | $\theta_{\text{cluster}}^b$ (deg) |
|--------------|----------------------------------|-----------------|--------------------------------------|
| MKW 1 | 46 ± 3 | 0.28 | 50 |
| MKW 2 | 41 ± 2 | 0.22 | 60 |
| MKW 4 | 101 ± 1 | 0.30 | 120 |
| MKW 5 | 98 ± 5 | 0.13 | ... |
| MKW 6 | 106 ± 2 | 0.45 | 56 |
| MKW 7 | 168 ± 3 | 0.10 | 150 |
| MKW 8 | 103 ± 11 | 0.14 | 10 |
| MKW 9 | 55 ± 30 | 0.05 | ... |
| MKW 10 | 171 ± 4 | 0.40 | 175 |
| MKW 11 | 172 ± 8 | 0.25 | 165 |
| MKW 12 | 105 ± 7 | 0.14 | 65 |
| MKW 1s | 15 ± 1 | 0.24 | 140 |
| MKW 2s | 148 ± 2 | 0.10 | 130 |
| MKW 3s | 103 ± 1 | 0.21 | ... |
| MKW 4s | 30 ± 1 | 0.38 | 55 |
| AWM 1 | 65 ± 2 | 0.21 | 20 |
| AWM 3 | 92 ± 1 | 0.26 | ... |
| AWM 4 | 167 ± 1 | 0.25 | ... |
| AWM 5 | 82 ± 1 | 0.26 | ... |
| AWM 6 | 116 ± 4 | 0.45 | ... |
| AWM 7 | 69 ± 5 | 0.20 | ... |

^a Position angles were measured north through east.

^b Cluster position angles from Flin et al. 1995.

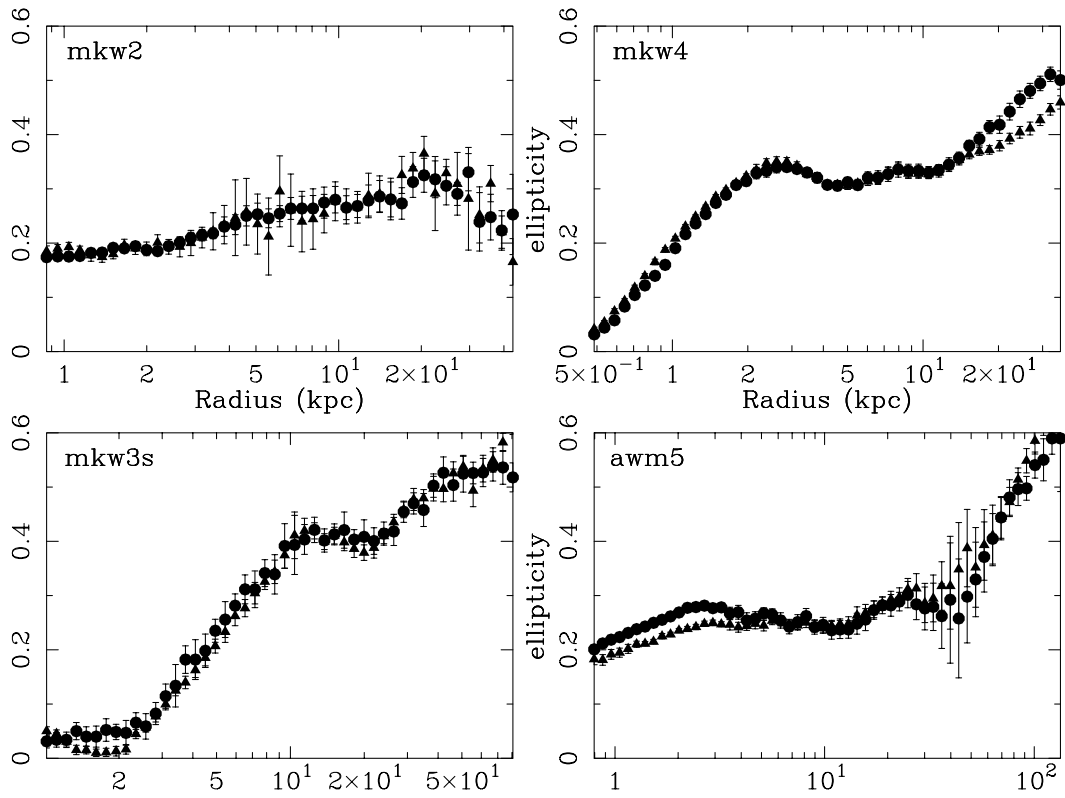


FIG. 2.—Ellipticity vs. radius (in units of kiloparsecs) profile measured in *B* (circles) and *R* (triangles) for a sample of the AWM/MKW poor cluster BCGs.

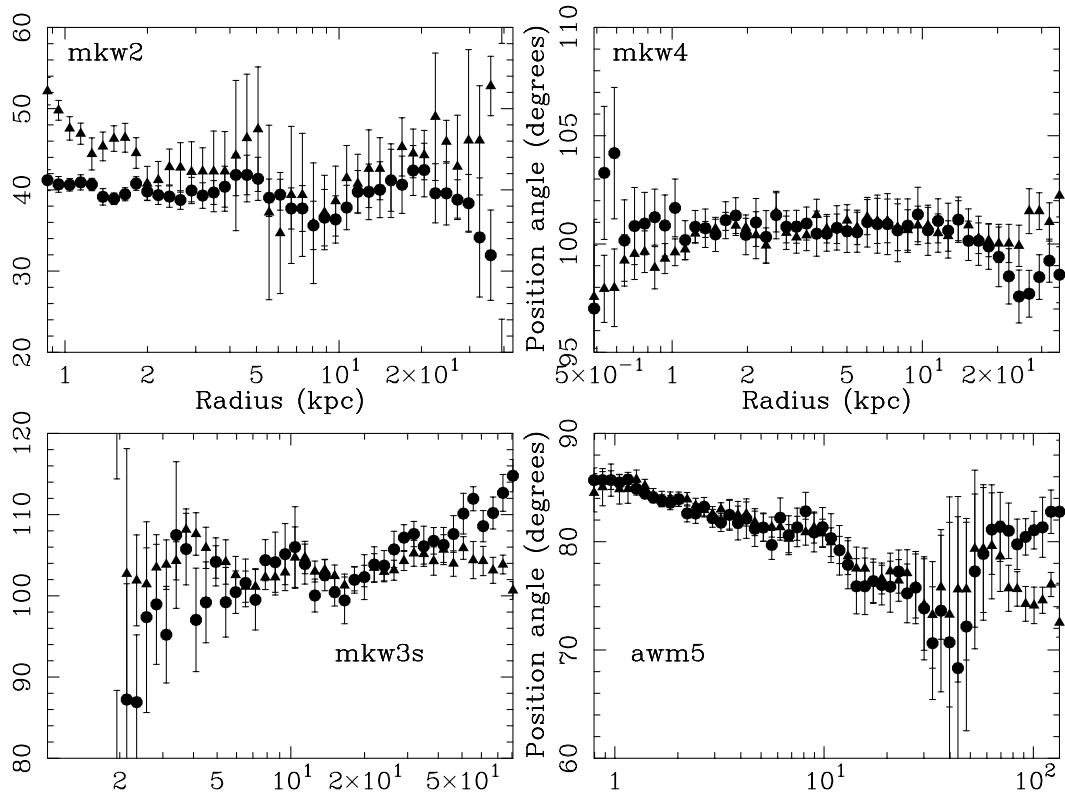


FIG. 3.—Position angle versus radius (in units of kiloparsecs) profile measured in *B* (circles) and *R* (triangles) for a sample of the AWM/MKW poor cluster BCGs.

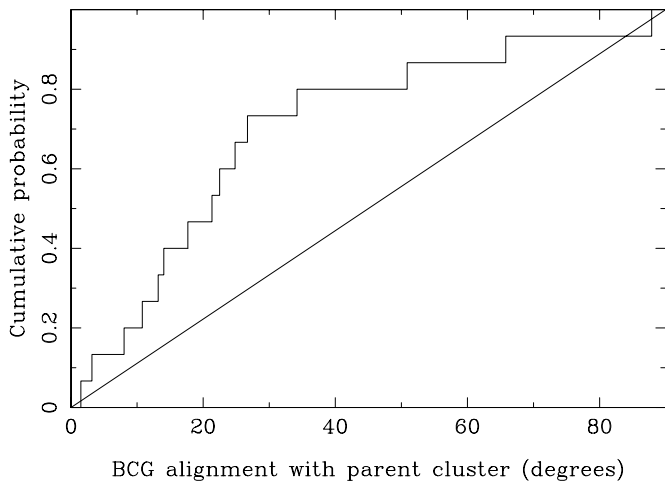


FIG. 4.—Cumulative probability distribution of the angle between BCG major axis and host cluster principal axis; the straight line is that expected for a random distribution. The K-S test shows that poor cluster BCGs are aligned within their host clusters at the 92% confidence level.

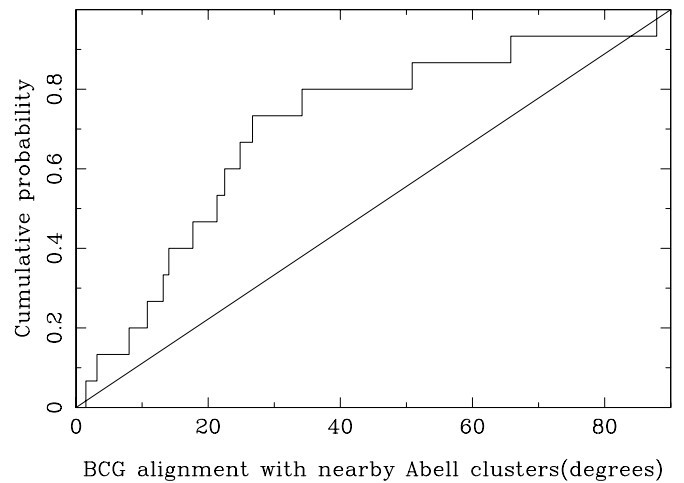


FIG. 5.—Cumulative probability distribution of the acute angle between the BCG major axis and the great circle connecting the galaxy with a neighboring Abell cluster within $20 h^{-1}$ Mpc. The observed distribution (*stepped line*) shows a clear departure from a random distribution (*straight line*) at the 99% confidence level.

played significant isophotal twisting. The largest degree of twisting was $\sim 20^\circ$ in AWM 3, which is much smaller than the 40° twists found by Porter, Schneider, & Hoessel (1991) in a sample of bright elliptical galaxies.

To determine if the BCG position angles were aligned with their parent clusters, we applied the Kolmogorov-Smirnov (K-S) test. We discarded any galaxies with mean position angle errors of $\geq 15^\circ$ or mean ellipticities $(1 - b/a)$ of less than 0.2, since round galaxies do not have well-defined major axes. After application of these limitations there were nine BCG-parent cluster pairs. Figure 4 shows the cumulative probability distribution as a function of the alignment angle between the BCGs and their parent clusters and for a random distribution of angles. The cluster position angles were taken from Flin et al. (1995). Since the alignment angles must be sorted according to size to apply the K-S test and random angles are all equally probable, the cumulative probability distribution for a random set of angles is a straight line with a slope of 1. The BCG position angles clearly show a departure from a random distribution. The K-S test allows us to reject the hypothesis that the alignment angles come from a random distribution at the 92% level. Thus we may say with confidence that the major axes of poor cluster dominant galaxies are aligned with their parent clusters, in agreement with Flin et al. (1995).

Next, we located the Abell clusters within $20 h^{-1}$ Mpc and measured the acute angle between the BCG major axis and the great circle connecting the galaxy with the Abell cluster. There were 10 MKW/AWM clusters meeting the position angle and ellipticity restrictions that had one or more neighboring Abell clusters; in all there were 15 galaxy-Abell cluster pairs. Figure 5 shows the cumulative probability distribution for the angle between the BCG major axis and the principal axis of the host cluster. The K-S test shows that the distribution is nonrandom at the 99% level. Hence these results indicate that BCGs in poor clusters are as strongly aligned with their environs as are their counterparts in richer Abell clusters (see, e.g., West 1994).

The K-S test does not take into consideration the errors in the position angles, so we performed a series of 1000 K-S

tests on data generated by adding random deviations of $\pm 15^\circ$ to the measured position angles. This value was chosen because it is one of our criteria for rejection of position angles and is a generous error allowance. The median significance level of the 1000 K-S tests for the BCG-parent cluster data was $92.3\% \pm 8\%$ and $98.9\% \pm 1\%$ for the BCG-Abell cluster data (errors are $\pm 1 \sigma$). This robust test demonstrates that the alignment effect is not easily masked by variations of up to 15° in the position angles.

A K-S test using only those Abell clusters within $10 h^{-1}$ Mpc was inconclusive, owing to the small sample size, because there are relatively few neighboring clusters within this separation. When all Abell clusters within $30 h^{-1}$ Mpc were included, no significant departures from randomness were found.

4. DISCUSSION

The observed alignments of BCGs, clusters, and superclusters—a coherence of structures over scales from tens of kiloparsecs to tens of megaparsecs—must surely be an important clue about how these objects formed. The results presented in this paper provide an important new piece of information: whatever mechanism is responsible for producing alignments of BCGs with their surroundings, it appears to operate equally well in both rich and poor clusters.

We believe that these alignments are readily explained by hierarchical models of structure formation in which BCGs and clusters are built by infall of material that flows along the filamentary superclusters in which they are embedded. In such a scenario, clusters and their brightest member galaxies are built by a series of mergers that occur preferentially along the direction defined by the filament, and hence these objects will naturally develop orientations that reflect the surrounding filamentary pattern of superclustering. In this way the matter distribution on supercluster scales influences the properties of clusters and their BCGs. Such a process would be expected to produce alignments of BCGs in both poor and rich clusters.

This picture of cluster and BCG formation via anisotropic mergers is strongly supported by theoretical work and numerical simulations, which have shown that infall of material into clusters along filaments is a generic feature of most gravitational instability models of structure formation. (e.g., Bond 1987; Bond, Kofman, & Pogosyan 1996; van Haarlem & van de Weygaert 1993; West 1994; Dubinski 1998). Observational evidence also supports this idea; for example, West, Jones, & Forman (1995) showed that the distribution of merging subclusters in clusters—the building blocks from which rich clusters are made—traces the surrounding filamentary distribution of matter on supercluster scales. Assuming that BCGs formed by mergers, then it is natural to expect that such mergers will also occur preferentially along the direction defined by the cluster principal axis, which is itself dictated by the surrounding filamentary mass distribution on supercluster scales.

The fact that BCGs in poor clusters exhibit the same alignment effect that is seen in the richer Abell clusters indicates that this alignment phenomenon is not limited to the most massive galaxy clusters. The possibility that such

galaxy alignments might extend to even sparser groups is worth exploring.

5. SUMMARY

We have shown that the brightest member galaxies in poor MKW/AWM clusters are preferentially aligned with the principal axes of their host clusters and that they also point toward nearby rich clusters. BCG–parent cluster alignments and BCG–nearby cluster alignments are observed in both poor and rich clusters, and furthermore the degree of alignment is very significant in both types of clusters. These two observations assert that cluster richness cannot be a factor in producing alignments. We suggest that these alignments are most likely produced by formation of (rich and poor) cluster BCGs by infall along filamentary structures, which are a generic feature of many models for the formation of large-scale structure.

M. J. W. and T. M. F. were supported by a grant from NSERC of Canada.

REFERENCES

- Albert, C. E., White, R. A., & Morgan, W. W. 1977, *ApJ*, 211, 309
 Beers, T. C., Kriessler, J. R., Bird, C. M., & Huchra, J. P. 1995, *AJ*, 109, 874
 Binggeli, B. 1982, *A&A*, 107, 338
 Bond, J. R. 1987, in *Nearly Normal Galaxies: From the Planck Time to the Present*, ed. S. Faber (New York: Springer), 388
 Bond, J. R., Kofman, L., & Pogosyan, D. 1996, *Nature*, 380, 603
 Carlberg, R. G., Yee, H. K. C., Ellingson, E., Abraham, R., Gravel, P., Morris, S., & Pritchet, C. J. 1996, *ApJ*, 462, 32
 Carter, D., & Metcalfe, J. 1980, *MNRAS*, 191, 325
 Dubinski, J. 1998, *ApJ*, 502, 141
 Flin, P., Trevese, D., Krywult, J., & Cirimele, G. 1995, *SESTO Meeting, Observational Cosmology*, 1995 July
 Jedrzejewski, R. I. 1987, *MNRAS*, 226, 747
 Lambas, D. G., Groth, E. J., & Peebles, P. J. E. 1988, *AJ*, 95, 996
 Lambas, D. G., Mariano, N., Muriel, H., & Ruiz, L. 1990, *AJ*, 100, 1006
 Morgan, W. W., Kayser, S., & White, R. A. 1975, *ApJ*, 199, 545
 Porter, A. C., Schneider, D. P., & Hoessel, J. G. 1991, *AJ*, 101, 1561
 Rhee, G. F. R. N., & Katgert, P. 1987, *A&A*, 183, 217
 Sastry, G. N. 1968, *PASP*, 83, 313
 Struble, M. F. 1990, *AJ*, 99, 743
 Struble, M. F., & Peebles, P. J. E. 1985, *AJ*, 99, 743
 Trevese, D., Cirimele, G., & Flin, P. 1992, *AJ*, 104, 935
 van Haarlem, M., & van de Weygaert, R. 1993, *ApJ*, 418, 544
 West, M. J. 1994, *MNRAS*, 268, 79
 West, M. J., Jones, C., & Forman, W. 1995, *ApJ*, 451, L5
 Zabludoff, A. I., Geller, M. J., Huchra, J. P., & Vogeley, M. S. 1990, *ApJS*, 74, 1